E3S Web of Conferences **601**, 00102 (2025) https://doi.org/10.1051/e3sconf/202560100102
ICEGC'2024

Nonlinear control design of a DC microgrid based on the integral sliding mode controller

Hajar Akli[1,*], *Hassan* Abouobaida[1], *Youssef* Mchaouar[1], *Abdelmoghit* Fathelkhair[1], and *Khadija* Oualifi[1]

[1]LabSIPE at National School of Applied Sciences, Chouaib Doukkali University, EL Jadida 24002, Morocco

Abstract.
This article is designed to control the stability and the effective operation in a different entity of DC microgrid(MG) under varying climatic and load conditions. The proposed MG contains primarily renewable sources including photovoltaics (PV) commanded by a DC-DC boost converter additionally the wind power conversion system with a turbine wind, a permanent magnet Synchronous Generator (PMSG), a three-phase diode rectifier, and ultimately a DC-DC buck-boost converter. In addition, this system also includes a battery energy storage system (BESS) with a bidirectional DC-DC. The last component is the variable DC charge. The general purposes of this paper are the following firstly, obtaining the maximum power from PV and wind energy by using the perturb and observation method and by operating the boost converter and the buck-boost. Second, maintain the DC bus voltage as a constant value. Lastly, the management of energy and storage by controlling the bidirectional converter. The structure of energy conversion is elaborated by the mathematical model, controlled by a nonlinear technique which is the integral sliding mode control (ISMC). The robustness, performance, and efficiency are demonstrated with a simulation in MATLAB/SIMULINK.

1 Introduction

The constant evolution of the energy sector has led to the development of innovative solutions to meet the growing demand for electric energy while adhering to a set of key parameters. The concept of microgrid (MG) has recently gained popularity due to its ability to integrate distributed renewable energy resources, such as photovoltaic and wind systems, efficiently and reliably [1]. Depending on the voltage of the connected bus, MG can be represented as a DC, AC, or hybrid AC/DC MG type [2]. With the rising presence of DC-output renewable energy sources and DC loads in MG, DC MG has progressively gained attention as a more appropriate power supply mode for integrating DC components, providing greater stability and commandability, which can solve the problem of fluctuating renewable energy output on the distribution grid [3].

It is widely recognized that wind turbines and photovoltaic (PV) units are the most popular renewable energy sources (RES) in an MG, with their varying power according

*e-mail: haajaarakli@gmail.com

to irradiance and wind speed. Moreover, the Battery Energy Storage System (BESS) has become a crucial element of MG, as it helps to stabilize RES fluctuations by keeping the excess energy and discharging it based on load requirements and also can help to maintain a stable voltage on the DC bus [4], [5]. Successful control of a DC MG, is necessary to manage these converters Effectively [6].

The integral sliding mode control (ISMC) is a nonlinear control method, that offers a different advantage, including robustness, fast response, elimination of external perturbations, and an easy implementation [7]. This article aims to design and implement an Integral Sliding Mode Controller (ISMC) to optimize the operation of a microgrid that includes photovoltaic (PV) panels, wind turbines, and Battery Energy Storage Systems (BESS). The study seeks to improve the microgrid stability and reliability by ensuring that the ISMC effectively manages the variation of power from the PV panels, wind turbine, and DC load while optimizing the use of the BESS for energy storage. The article will also assess the ISMC's robustness against disturbances and uncertainties through simulations to validate its performance across various weather and load demand conditions. All the diver's objective is obtained by the implementation of ISMC, firstly, for the boost converter with the PV generator to maintain that the voltage output of the PV panel follows the reference, which is obtained with the MPPT. In addition, the regulation of the buck-boost converter in order to get an optimal angular speed that is generated by the MPPT. And finally, the control of the bidirectional DC-DC converter ensures the stability of the DC-bus at the desired value. The structure of this article is presented in Section 2, also in this section, we will present the configuration and the model of the isolated DC MG. The objectives and the conception of the nonlinear controls for all the components are presented in Section 3. The simulation results are developed in Section 4, and a conclusion is submitted at the end.

2 System configuration and modeling

The following figure represents the general structure of our DC MG, which is composed of a photovoltaic unit connected to the DC bus with a DC-DC boost converter bias and a wind power generation connected to the DC bus through a diode rectifier and DC-DC buck-boost converter. Additionally, a BESS unit is utilized, and it is connected to the DC bus through a Bidirectional DC-DC converter, which can operate in charging or discharging mode respectively to the charge demand. Variable DC charge is connected to the DC bus. The DC bus has a Nominal voltage of 200 V.

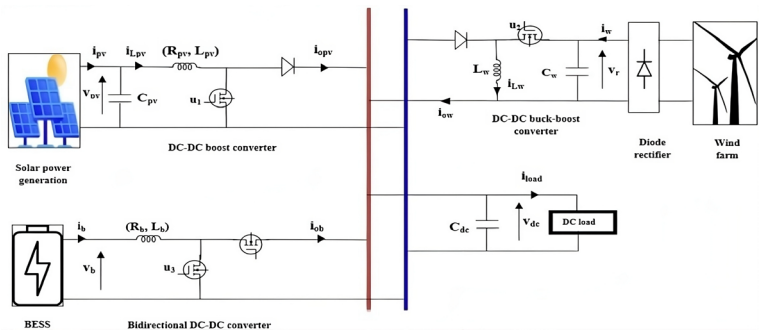

Figure 1. The general structure of MG.

2.1 Functional principle

The proposed MG operates in Island mode, the DC bus voltage and the power stability are maintained by a bidirectional DC-DC converter based on a different operation in the MG. Power should be regulated under varying load demands, which can be presented as follows:

$$P_{wind} + P_{pv} + P_{battery} = P_{Load} \tag{1}$$

Where P_{wind}, P_{pv} ,$P_{battery}$ and are used to express the power of the wind generator, PV generator, power of battery and power of DC load respectively. The dynamical model of all the components of our MG are presented in the following sections.

2.2 Modeling of PV unit with the DC-DC boost converter

Based on Fig.1, the dynamical model of the PV system related to the DC-DC boost converter can be illustrated by the succeeding differential equations. [8]:

$$\frac{dv_{pv}}{dt} = \frac{1}{C_{pv}}.(i_{pv} - i_{Lpv}) \tag{2}$$

$$\frac{di_{Lpv}}{dt} = \frac{1}{L_{pv}}.(v_{pv} - i_{Lpv} - R_{pv}.i_{Lpv} - (1 - u_1).v_{dc}) \tag{3}$$

Where v_{pv} is the output voltage and i_{pv} is the output current of the PV unit, $i_{Lpv}$is input current, C_{pv} represent the filtering capacitor, R_{pv} is the internal resistor and i_{pv} is internal inductor of the boost converter,u_1 is the PWM input control signal, v_{dc} illustrate the DC-bus voltage and C_{dc} is the DC-bus capacitor.

2.3 Modeling wind turbine and PMSG with a buck-boost converter

The aerodynamic power obtained from the wind turbine is expressed in by the mathematical relations below [9]:

$$P_a = \frac{1}{2}.C_p(\lambda,\beta).\phi.\pi.R^2.v_v^3 \tag{4}$$

$$\lambda = \frac{\Omega.R}{v_v} \tag{5}$$

Where v_v is the wind speed, C_p is the power coefficient, R is the blade radius, β represent the pitch angle, is the tip speed ratio, Ω is angular speed and ϕ is the air density. Equation.5 shows that the power will reach its maximum for a given wind speed when the power coefficient C_p = $C_{p,max}$. The power coefficient of the turbine is a non-linear function of λ and β [10].

$$C_p = 0,576.(\frac{116}{\lambda} - 0,4.\beta - 5)\exp^{\frac{-21}{\lambda_i}} \tag{6}$$

$$\frac{1}{\lambda_i} = \frac{1}{\lambda + 0.08.\beta}.\frac{0,035}{\beta^3 + 1} \tag{7}$$

For =0, $\beta = 0$ the maximum power coefficient takes the following value C_p= 0.5278 which is equivalent to $\lambda_{optimal}$= 8.016. The PMSG modeling in two-phase reference d-q is presented in [11].

The rotational dynamic law for the mechanical shaft is the following:

$$J.\frac{d\Omega}{dt} = T_m - T_{em} - f\Omega \tag{8}$$

Where T_m is the mechanical torque, T_{em} is the electromagnetic torque, J is the inertia and f is the viscous damping. The dynamic model of PMSG in the two-phase d-q reference frame is developed in [12]. As shown in Fig.1 the AC power which is generated by the PMSG is converted through a diode rectifier to DC power. Subsequently, this power is delivered to the DC-bus via the DC-DC buck-boost converter. Consequently, the dynamic model of the buck-boost converter is characterized as follows [13].

$$\frac{dv_r}{dt} = \frac{1}{C_m}.(i_r - u_2.i_{Lw}) \tag{9}$$

$$\frac{di_{Lw}}{dt} = \frac{1}{L_w}.(u_w.v_r - (u_2 - 1).v_{dc}) \tag{10}$$

Where the v_r is output DC voltage of the diode rectifier and i_{Lw} is the current witch crosses the L_w inductance and u_2 is the PWM input control signal. Remark 1. The optimal angular speed method is used in this article to obtain the MPPT due to its rapidity and simplicity [9].

2.4 Modeling the BESS unit with the bidirectional DC-DC converter

The fig.1 depicts the electrical circuit of the BESS unit in combination with the bidirectional DC-DC converter. The dynamic model of this converter is the following [5]:

$$\frac{di_b}{dt} = \frac{1}{L_b}.(v_b - R_b.i_b - u_3.v_{dc}) \tag{11}$$

$$\frac{dv_{dc}}{dt} = \frac{1}{C_{dc}}.((1 - u_3).i_b - i_{load} + i_{opv} + i_{ow}) \tag{12}$$

Where v_b is the battery's output voltage, i_{ob} is the converter output current, L_b and R_b are the inductance and the resistor successively and u_3 is the input of control for bidirectional converter. The dynamical models of the different MG components are used to design the controllers; the full controller design process is covered in the following section. Remark 2. In this article, we will use a lithium-ion battery and constant voltage (CV) mode [14].

3 Control structure design

The principal objectives for the ISMC are to reduce the steady-state error and to improve the robustness. The proposed ISMC in this section aims to generate the PWM input control signals for all the converters in our MG architecture. These subsections present the ISMC design for all the components in our MG.

3.1 Control design for the boost converter with PV unit

The main objective of the boost converter interfaced control is to maintain the output voltage of the PV generator at the reference value v^*_{pv}, which is specified by the perturb and observe MPPT algorithm. the proposed sliding surface is:

$$S_1 = K_1.e_1 + K_2.\int e_2 \tag{13}$$

Where K_1 and K_2 are a positive constants and e_2 is steady-state error witch equals :

$$e_1 = v_{pv} - v_{pv}^* \tag{14}$$

Let's examine the Lyapunov function and its derivative:

$$V(S_1) = \frac{1}{2}.S_1^2 \tag{15}$$

$$V(S_1) = S_1.S_1 \tag{16}$$

From the equations.2 and 3 we found:

$$S_1 = \frac{K_1}{C_{pv}}.(i_{pv} - i_{Lpv}) + K_2.[v_{Lpv} + R_{pv}.i_{pv} + (1 - u_1).v_{dc} - v_{pv}] \tag{17}$$

$$V(S_1) = S_1[\frac{K_1}{C_{pv}}.(i_{pv} - i_{Lpv}) + K_2.[v_{Lpv} + R_{pv}.i_{pv} + (1 - u_1).v_{dc} - v_{pv}]] \tag{18}$$

The condition of stability is $V(S_1) < 0$

Let's choose the control law S_1 such that the time derivative of are governed by:

$$S_1 = -K_3.sign(S_1) \tag{19}$$

according to equations.17 and 19,the general law command is:

$$u_1 = \frac{1}{v_{dc}}.[(v_{Lpv} + R_{pv}.i_{Lpv} - v_{pv}^*) + \frac{K_1}{K_2.C_{pv}}.(i_{pv} - i_{Lpv}) + \frac{K_3}{K_2}.sign(S_1)] \tag{20}$$

3.2 Regulation design for the buck-boost converter interfaced with the wind generator

The major goal of DC-DC buck-boost converter regulation is to preserve the following reference angular speed $\Omega_{optimal}$ by the MPPT algorithm and to maintain the output voltage of diode rectifier at the reference value . The proposed sliding surface is:

$$S_2 = K_4.e_2 + K_5.\int e_3 \tag{21}$$

Where K_4 and K_5 are a positive constants and , are the steady-state errors witch equals :

$$e_2 = v_r - v_r^* \tag{22}$$

$$e_3 = \Omega - \Omega_{optimal} \tag{23}$$

Remark 3. The electrical power P_r at the output of the diode rectifier, in the case of a negligible joule losses is equal to:

$$P_a = -P_r = v_r.i_r \tag{24}$$

Where is P_a the power extracted with the turbine, then the calculation formula of the voltage reference v_r^* is:

$$v_r^* = \frac{-Pa}{i_r} \tag{25}$$

Remark 4. We applied the same Lyapunov stability demonstration as previously discussed in part 3.1. on the wind generator with buck-boost converter, we found the following general command law:

$$u_2 = \frac{i_r}{i_{Lw}} + \frac{C_w}{K_4.i_{Lw}}.[K_6.sign(S_2) + K_5.e_3] \tag{26}$$

Where is positive constant.

3.3 Regulation design for the bidirectional DC-DC converter of BEES

The primary purpose of the bidirectional DC-DC converter control is to regulate the DC-bus voltage at the desired value (v_{dc}^{*}=200V) and to manage the power demand between the power generators and the variable power load. The ISMC control strategy applied is the following:

We define the steady-state error with:

$$e_4 = v_{dc} - v_{dc}^{*} \tag{27}$$

Defining the sliding surface:

$$S_3 = K_7.e_4 + K_8.\int e_4 \tag{28}$$

Where K_7 and K_8 are a positive constants.Remark 5. We applied the same Lyapunov stability demonstration as previously discussed in part 3.1. on the BEES with a bidirectional DC-DC converter, we found The general law command is:

$$u_3 = 1 + \frac{i_{opv} + i_{ow} + i_{load}}{i_b} + \frac{C_{dc}}{K_7.i_b}.[K_8.e_4 + K_9.sign(S_3)] \tag{29}$$

Remark 6.The global Lyapunov function is the sum of the Lyapunov function for the three systems, the following function present V_{global}:

$$V_{global} = \Sigma_i^{i=1,2,3}\ V(S_i). \tag{30}$$

$$V_{global} = \frac{1}{2}.\ \Sigma_i^{i=1,2,3}\ S_i^2. \tag{31}$$

The derivative of the Lyapunov function is:

$$V_{global} = \frac{1}{2}.\ \Sigma_i^{i=1,2,3}\ S_i.S_i. \tag{32}$$

The condition of stability is $V_{global} < 0$
The global sliding mode control law is presented by:

$$S_{global} = -K_3.sign(S_1) - K_6.sign(S_2) - K_9.sign(S_3) \tag{33}$$

By substituting equation (32) in equation (31) we found:

$$V_{global} = S_1(-K_3.sign(S_1)) + S_2(-K_6.sign(S_2)) + S_3(-K_9.sign(S_3)) \tag{34}$$

Since $S_i.sign(S_i) = |S_i|$ with (i=1,2,3) and the $|S_i|$ is the absolute value of S_i the equation become:

$$V_{global} = (-K_3.|S_1| - K_6.|S_2| - K_9.|S_3|) \tag{35}$$

We have K_3, K_6, K_9 are positive constants and $|S_1|, |S_2|, |S_3|>0$ .This shows that $V_{global} < 0$ that improve the system stability.

4 Examination of the controller performance

The performance examination of the proposed control structure for our isolated DC MG, as illustrated in Fig.1, was done in MATLAB/SIMULINK software. The control parameters, DC block diagram, and multiple case studies of the test MG system are presented in the following subsections.

	Parameters	Values or Type
PV generator	Photovoltaic module	1Soltech 1STH-215-P
	Parallel strings, series-connected	14 , 4
	ximum output power P_{pv}	10.43 kw
	C_{pv} , L_{pv}, R_{pv}	200 μF,5mH,10 mΩ.
Wind unit	R,v_v,P_{wind}	4 m ,12 m/s, 25.5 kW
PMSG	R_s,L_d,L_q	50 m, 0.6 mH
	ϕ_f	1.7 V.s
	C_w,L_w	500 μF, 1 mH
Battery lithium	v_b,Q_b	100 V, 100 Ah
	R_b,L_b	1mΩ, 10 mH
	v_{dc}	200 V
	C_{dc}	5000 μ.F
	DC Load	10 Ω, 6 Ω

Table 1. Electrical parameters of DC microgrid.

4.1 Simulation parameters

The following table (Table.1) presents the set of electrical parameters for the DC microgrid:

The following table shows the ISMC parameters control: In this work, to confirm the

f (PWM)	10 KHz
DC-DC boost converter (ISMC)	K_1=40 ,K_2=50 ,K_3=100
DC-DC buck-boost converter (ISMC)	K_4=1.33*10^{-12} ,K_5=10^{-12} ,K_6=2.10^5
Bidirectional DC-DC converter ISMC	K_7=10^{-8} ,K_8=10^{-6} ,K_9=2.10^4

Table 2. ISMC parameters.

efficacy of the developed controller in regulating the DC-bus voltage while delivering power to load, we chose a diver state of a variable generation and load power in the following subsection. The variable weather conditions during the simulation are presented in the following table:

	Time (s)	0 -0.7	0.7 - 1	1 - 2	2 - 2.5
PV generator	Solar irradiation(w/m²)	1000	200	200	200
	Temperature (deg)	25	25	25	25
Wind unit	Wind speed (m/s)	10	10	8	8

Table 3. Weather conditions.

4.2 Simulation results

The following figure shows the regulation results of PV output voltage, before 0.7s with an irradiance equals to 1000 (w/m2) the voltage closely follows the reference voltage v_{pv} . After an irradiance change to 200 (w/m2) at 0.7s, fluctuations increase but remains near the reference For the wind regulation, the results of the simulation for the angular speed and

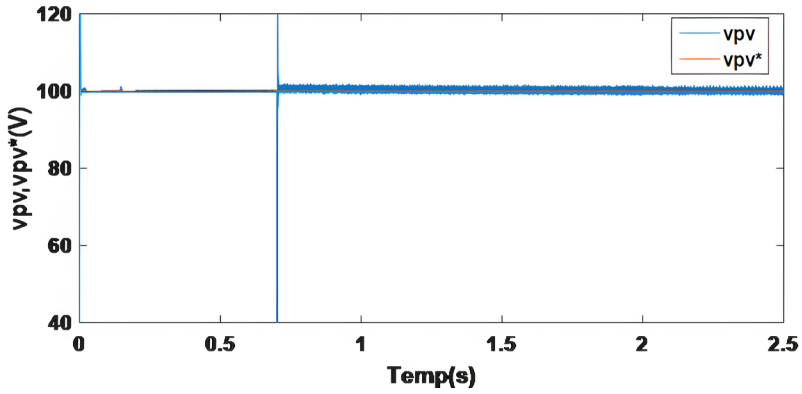

Figure 2. PV voltage.

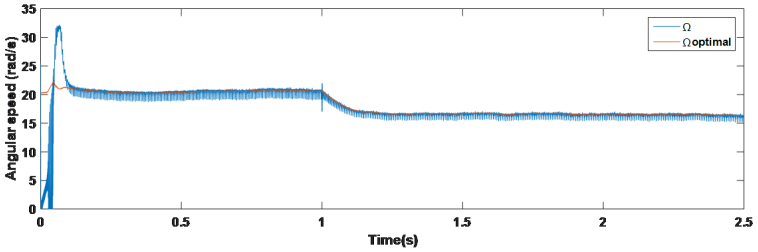

Figure 3. Mechanical speed (rad/s).

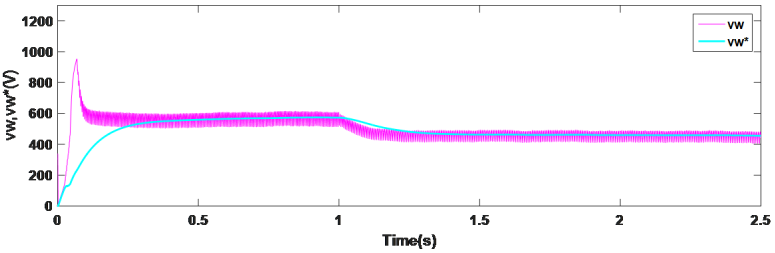

Figure 4. The rectifier output voltage.

output voltage of the rectifier are shown in the following figures respectively:

The angular speed in Fig.3 illustrates precise tracking of the optimal speed generated by the MPPT. Similarly, in Fig.4 the voltage output follows its reference, maintaining consistent regulation despite the variation in wind speed from 10m/s to 8m/s. This shows the robustness of the ISMC, ensuring that both mechanical and electrical parameters adjust effectively to changes in wind conditions.

For the simulation results for the BESS unit with the bidirectional DC-DC converter, the following figures show the variation of power flow under the weather the demand of load

during the time, and the DC-bus voltage respectively: The following table presents a full

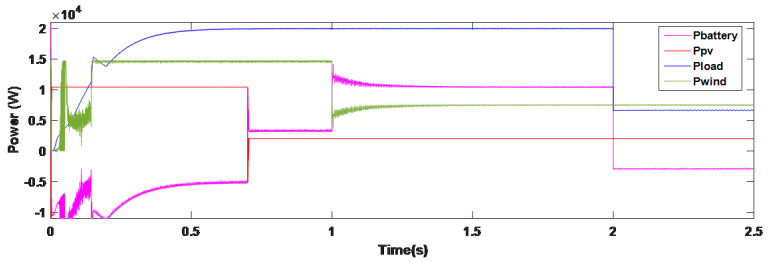

Figure 5. Powers.

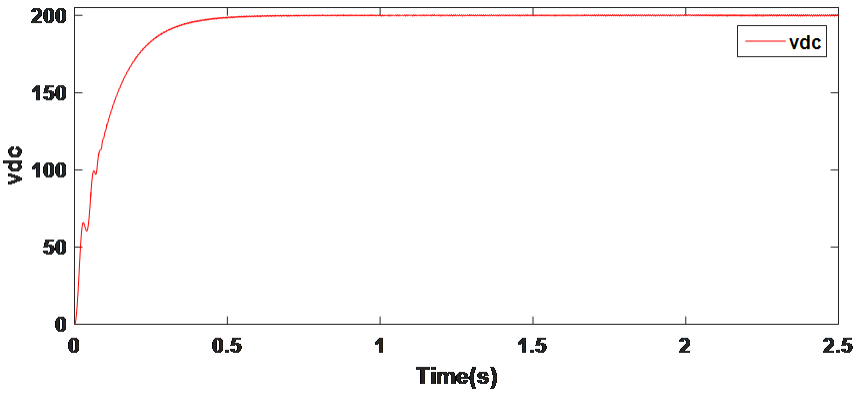

Figure 6. Common DC-bus voltage.

overview of the set variation for power during the time: Fig.5 and Fig.6 show that the bus

	Time (s)			
Power flows (Kw)	0 -0.7	0.7 - 1	1 - 2	2 - 2.5
P_{pv}	10.43	2.050	2.050	2.050
P_{wind}	14.7	14.7	7.560	7.560
$P_{battery}$	-5130	3250	10.39	-2944
P_{load}	20	20	20	6.666

Table 4. Power flow.

voltage regulation accurately tracks the reference value of 200V, showcasing the performance of the ISMC. Additionally, energy management between demand and generation is efficiently maintained through the bidirectional DC-DC converter, which enables the battery to adjust to energy fluctuations by either charging or discharging as required, thereby ensuring microgrid stability.

5 Conclusion

In conclusion, the implementation of ISMC has effectively achieved all the set objectives, proving its capability to optimize the performance of our MG system. Through the application of ISMC to the boost converter connected to the PV generator, the output voltage was accurately regulated to track the reference derived from the MPPT algorithm. Moreover, the buck-boost converter was successfully managed to maintain the optimal angular speed of the wind turbine, ensuring maximum power extraction. Finally, the bidirectional DC-DC converter effectively stabilized the DC-bus voltage at the desired level, enhancing the overall stability of the microgrid under varying weather conditions. Simulations confirmed the ISMC resilience and fast response, making it a robust control method for managing power fluctuations from renewable energy sources and optimizing the use of Battery Energy Storage Systems (BESS).

Funding

This work was carried out with the support of the National Center for Scientific and Technical Research (CNRST) as part of the "PhD-Associate Scholarship- PASS" program.

References

[1] M. Shaban, M. A. Mosa, A. A. Ali, et K. M. Abdel-Latif, "Effect of power sharing control techniques of hybrid energy storage system during fault conditions in DC microgrid," Journal of Energy Storage, vol. 72, p. 108249, Nov. 2023, doi: 10.1016/j.est.2023.108249.

[2] R. Sepehrzad, J. Ghafourian, A. Hedayatnia, A. Al-Durrad, et M. H. Khooban, "Experimental and developed DC microgrid energy management integrated with battery energy storage based on multiple dynamic matrix model predictive control," Journal of Energy Storage, vol. 74, p. 109282, Dec. 2023, doi: 10.1016/j.est.2023.109282.

[3] X. Zhu, D. Wang, J. Li, C. Li, M. Liu, et B. Zhao, "Online optimization and tracking control strategy for battery energy storage in DC microgrids," Journal of Energy Storage, vol. 73, p. 108919, Dec. 2023, doi: 10.1016/j.est.2023.108919.

[4] Z. Ullah et al., « Implementation of various control methods for the efficient energy management in hybrid microgrid system », Ain Shams Engineering Journal, vol. 14, no 5, p. 101961, mai 2023, doi: 10.1016/j.asej.2022.101961.

[5] T. K. Roy, S. K. Ghosh, et S. Saha, « Stability enhancement of battery energy storage and renewable energy-based hybrid AC/DC microgrids using terminal sliding mode backstepping control approaches », ISA Transactions, vol. 142, p. 40-56, nov. 2023, doi: 10.1016/j.isatra.2023.07.014.

[6] F. Rezayof Tatari, M. Banejad, A. Akbarzadeh Kalat, et G. Iwanski, « A long-horizon move-blocking based direct power model predictive control for dynamic enhancement of DC microgrids », Ain Shams Engineering Journal, vol. 15, no 7, p. 102837, juill. 2024, doi: 10.1016/j.asej.2024.102837.

[7] Y. Mchaouar et al., « Nonlinear control of single stage grid-tied photovoltaic systems based on a 3L-NPC topology », IFAC-PapersOnLine, vol. 55, no 12, p. 538-543, 2022, doi: 10.1016/j.ifacol.2022.07.367.

[8] T. K. Roy, M. A. Mahmud, A. M. T. Oo, M. E. Haque, K. M. Muttaqi, et N. Mendis, « Nonlinear Adaptive Backstepping Controller Design for Islanded DC Microgrids », IEEE Trans. on Ind. Applicat., vol. 54, no 3, p. 2857-2873, mai 2018, doi: 10.1109/TIA.2018.2800680.

[9] H. Abouobaida et S. E. Beid, « The Ripple Correlation Optimal Point Determination in a Medium Power Wind Conversion System and Performance Evaluation with Respect to Conventional Algorithms », in Modeling, Identification and Control Methods in Renewable Energy Systems, N. Derbel et Q. Zhu, Éd., Singapore: Springer, 2019, p. 131-150. doi: 10.1007/978-981-13-1945-7-6.

[10] P. Gajewski et K. Pieńkowski, « Analysis of Sliding Mode Control of variable speed wind turbine system with PMSG », in 2017 International Symposium on Electrical Machines (SME), juin 2017, p. 1-6. doi: 10.1109/ISEM.2017.7993554.

[11] A. Archana et L. Arun, « Synthesis of sliding and integral sliding mode controllers for the VSC-HVDC transmission link », in 2017 IEEE International Conference on Signal Processing, Informatics, Communication and Energy Systems (SPICES), août 2017, p. 1-7. doi: 10.1109/SPICES.2017.8091333.

[12] A. Archana et L. Arun, « Synthesis of sliding and integral sliding mode controllers for the VSC-HVDC transmission link », in 2017 IEEE International Conference on Signal Processing, Informatics, Communication and Energy Systems (SPICES), Kollam: IEEE, août 2017, p. 1-7. doi: 10.1109/SPICES.2017.8091333.

[13] A. Fathelkhair, H. Abouobaida, Y. Mchaouar, Y. Abouelmahjoub, D. Elmesouli, et K. Oualifi, « Nonlinear Control for a Single Phase Grid Connected Wind Energy System », in Automatic Control and Emerging Technologies, Singapore : Springer Nature, 2024, p. 334-347. doi: 10.1007/978-981-97-0126-1-30.

[14] A. Watil, A. El Magri, R. Lajouad, A. Raihani, et F. Giri, « Multi-mode control strategy for a stand-alone wind energy conversion system with battery energy storage », Journal of Energy Storage, vol. 51, p. 104481, juill. 2022, doi: 10.1016/j.est.2022.104481.